Chapter 1

Introduction

1.1 Materials and Light

Light, earth (materials), and their interaction; these topics have been studied for thousands of years. The materials that make up our world truly are the "Substance of Civilization" [104]. In many ways, the history of our world has been defined by the materials we have had at our disposal. Many of the periods in human history have been characterized by the materials that were available: the stone age, the bronze age, the iron age, the industrial revolution (which came about in no small part from the development of manufactured steel), and the silicon age. Many periods of human advancement can be attributed to materials development for military and scientific applications. In addition, civilizations that had not developed militarily, historically fell victim to civilizations that had. As Tadahiro Sekimoto, former president of Nippon Electric Corporation, said:

> "Those who dominate materials, dominate technology."

This holds true for the future as well as the past. Recent research on plasmonics has demonstrated negative refraction at visible frequencies [66]. This advancement could lead to optical superlenses which may rival the best microscopes in existence today, as well as the possibility of "cloaking" objects from an outside observer [92]. Finally, work by Roddenberry et al. has looked at using dilithium crystals to travel faster than the speed of light [7]. Until that time comes, we must focus on materials currently available to us, and by far, the most prevalent optical material is glass.

1.2 Glass

In its most basic form, glass is a combination of silicon (the 2^{nd} most abundant material in the earth's crust) with oxygen (the most abundant material in the earth's crust). This simple combination is a key component in windows, computer chips, fiber optic cable, the sand at the beach,

optical telescopes, and a vast number of other applications. A metastable material, glass is basically a supercooled liquid frozen in place at room temperature. The fact that it's flowing, just extremely slowly, is evident from looking at the wavy windows in an old house or church that are actually thicker at the bottom than the top.

The first use of glass was not for optical purposes; rather, obsidian (volcanic glass which cools as it reaches the earth's surface) was cleaved into pieces and used as weapons and tools in the 7^{th} millennium B.C.E. The first evidence of glass making was around 3000 B.C.E. in an area called the Canaanite-Phoenician coast near the Mediterranean (just north of present-day Haifa). The sand from this region contained the right concentrations of lime and silica, so that the traders of this region needed only to mix in natron (a mix of soda ash, baking soda, salt, and sodium sulfate) while the melt was placed into a hot fire [104].[1]

The earliest glasses developed in this manner were opaque rather than transparent due to scattering from small air bubbles or particles trapped within the glass during formation. Later, during the 1^{st} millennium B.C.E., hotter kilns were developed and artisans began to introduce metal oxides into the glass to control the color. By forming the glass either with or without charcoal present, the glassworkers were able to either reduce or oxidize the copper, respectively, and as a result, produce glass that was either red or blue, respectively.

One of the most famous examples of metal being introduced into glass is the Lycurgus Cup. This glass was produced during the 4^{th} century A.D. during the Roman Empire (Figure 1.1). The cup depicts the death of King Lycurgus in Thrace at the hands of Dionysus. As can be seen from Figure 1.1, the glass appears red (a) when seen with light transmitted through the cup, and green (b) when seen with light reflected off the surface of the cup. This remarkable behavior results from the introduction of colloidal gold and silver into the glass during formation. The resulting gold-silver nanoparticles within the glass reflect the green portion of the visible spectrum while transmitting the red portion of the visible spectrum. A theory for this type of scattering from metal spheres would not be formalized until 1908 by Gustav Mie [72], $\simeq$ 2200 years after the cup was made.

It was not until the 13^{th} century that people began developing glass for scientific purposes and the idea of using glass to focus light became a reality. In the 1200s, the Italians invented eyeglasses

[1] Interestingly enough, around 1400 - 1300 B.C.E. the Phoenicians and Aramaeans of this trade route needed a method for recording all the financial information from their trades and as a result, developed the alphabetic language [104].

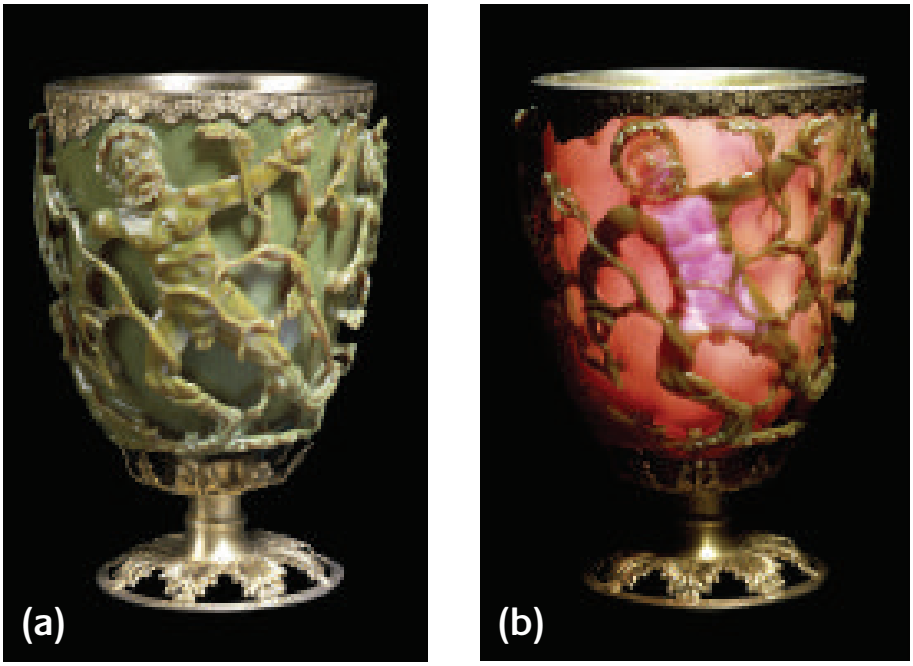

Figure 1.1. The Lycurgus cup shown in both reflection (a) and transmission (b). Gold-silver nanoparticles are responsible for the strong reflection of green light and transmission of red light [1].

which focused the direct and scattered light from objects whose sizes normally spanned millimeters to kilometers. At the end of the 16^{th} century, Hans Lippershey and Zacharias Jannsen produced two inventions that have changed the world. One, which was also developed by Jacob Metius, was the refracting telescope. A year later, an improved version was used by Galileo Galilei to focus light from the stars whose sizes spanned kilometers to billions of light years. Around the same time, with the help of Sacharias Jansen (Zacharias' dad), these men invented the microscope. Since then, this tool and its successors have focused light from millimeters down to nanometers.

Scientists have since been "focused" on exploring and manipulating nature on a smaller and smaller scale. Unfortunately, in the field of optics, this trend of ever smaller optics eventually reached a fundamental limit, diffraction. When the smallest dimension of an optical system, such as a waveguide, reaches $\frac{\lambda}{2n}$ where λ is the wavelength of the light and n is the refractive index of the waveguiding material, the device is diffraction limited. Below this limit, the waveguide will no longer be guided through the optical system. One method of getting around this diffraction limit that has evolved over the past 100 years, but has only taken off in the past 10, has been the field of plasmonics.

Plasmons have been studied since the beginning of the 20^{th} century. Sommerfeld and Zenneck

studied the effects of radio waves propagation along the surfaces of conductors in 1899 and 1907, respectively [106, 128]. As mentioned above, Gustav Mie published work on scattering from metal spheres in 1908 [72]. In 1957, Ritchie studied electrons at the surface of metallic films using electron energy loss spectroscopy [99], and in 1968, Ritchie published work on optical interactions with metallic gratings [100]. In the 1960's, methods for prisim coupling free-space light into surface plasmons was reported by Otto [82] as well as Kretschmann and Raether [60]. Since then, there have been thousands of papers published in the field of surface plasmons including the paper by Ebbesen et al. in 1998 which described enhanced optical transmission through sub-wavelength arrays [39]. This discovery was followed by the emerging field of "plasmonics" which is focused on developing device applications that utilize plasmonic effects.

1.3 Optical Properties of Materials

Any rigorous discussion of the interaction between light and materials begins with Maxwell's equations. In the absence of space charge and currents, we have:

$$\nabla \cdot \vec{E} = 0 \tag{1.1a}$$

$$\nabla \cdot \vec{B} = 0 \tag{1.1b}$$

$$\nabla \times \vec{E} = -\frac{1}{c}\frac{\partial \vec{B}}{\partial t} \tag{1.1c}$$

$$\nabla \times \vec{B} = \frac{1}{c}\varepsilon_i(\omega)\frac{\partial \vec{E}}{\partial t} \tag{1.1d}$$

In addition, we have the following constitutive relations for linear, non-magnetic materials:

$$\vec{D} = \epsilon_0 \epsilon \vec{E} \tag{1.2a}$$

$$\vec{B} = \mu_0 \mu \vec{H} \tag{1.2b}$$

$$\vec{P} = \epsilon_0 \chi \vec{E} \tag{1.2c}$$

where Equation 1.2a relates the dielectric displacement, $\vec{D}$, to the electric field, $\vec{E}$, through the dielectric constant, ϵ; Equation 1.2b relates the magnetic induction, $\vec{B}$, to the magnetic field, $\vec{H}$, through the permeability, μ; and Equation 1.2c relates the polarization, $\vec{P}$, to the electric field, $\vec{E}$, through the dielectric susceptibility, χ. In these equations, $\epsilon = \epsilon_1 + i\epsilon_2$ represents the complex

dielectric function of a material. While this representation of the material's optical constants is more explicitly used with Maxwell's equations, an equivalent form of this property is given by the complex index of refraction: $\tilde{n} = n + i\kappa$. Here, n is the ratio of the speed of light in vacuum to the speed of light in the material, and κ is the extinction coefficient of light within the material. This representation is more directly related to the experimental observation of light interacting with matter. Depending on the situation, the two equivalent forms will be used in this thesis, and related by:

$$\epsilon_1 = n^2 - \kappa^2 \tag{1.3a}$$

$$\epsilon_2 = 2n\kappa \tag{1.3b}$$

$$n = \sqrt{\frac{\epsilon_1}{2} + \frac{1}{2}\sqrt{\epsilon_1^2 + \epsilon_2^2}} \tag{1.3c}$$

$$\kappa = \frac{\epsilon_2}{2n} \tag{1.3d}$$

and κ is related to the absorption coefficient "α" of light propagating through a material by: $\alpha = \frac{2\kappa\omega}{c}$.

1.4 Metals

Traditionally, when materials are considered to design optical waveguides, metals are not the first thing that come to mind. Metals can be thought of as a sea of free electrons oscillating around a lattice of fixed ion cores. These electrons are free to move throughout the metal and respond when the metal experiences an applied external field. When exposed to an optical field at microwave and far-infrared frequencies, many metals behave like a perfect electrical conductor. The electrons are able to respond to the external stimulus with the same frequency as the applied field. This gives rise to the high reflectivities and negligible electromagnetic field penetration traditionally associated with metals. As the frequency of the field increases, so does the response of the electrons. For noble metals like gold, silver, and copper, this process continues up to visible frequencies. In this regime, metals reach a point of maximum oscillation where the driving field strongly couples into the longitudinal oscillations of the bulk electrons within the metal. This is known as the plasma frequency of the metal:

$$\omega_p = \sqrt{\frac{4\pi n e^2}{m^*}} \tag{1.4}$$

where "n" is the density of electrons within the metal and "m^*" is the effective mass of the electrons. Above this frequency, the metal behaves as a dielectric and experiences significant electromagnetic field penetration into the metal.

Separate from these "bulk plasmons" are a type of electron wave within metals known as a surface plasmon polaritons (SPPs). A SPP is a collective electron density oscillation at the interface between a metal and a dielectric; these SPPs will be the focus of this thesis. Hereafter, when the phrase "plasmon" is used, surface plasmon polaritons will be the intended meaning.

1.4.1 Dispersion and Surface Plasmons

Even though ϵ and $\tilde{n}$ are referred to as constants, in many situations, these properties can vary significantly depending on the configurations in which they are used as well as the frequency of the light involved. This property of materials is known as dispersion.

To calculate the dispersion of these structures, we start with an incident electromagnetic wave of the form:

$$\vec{E}(x,y,z) \sim E_0 \mathrm{e}^{i(k_x x - k_z|z| - \omega t)} \tag{1.5}$$

whose electric field has a perpendicular component to the waveguide (transverse-magnetic polarization). Here the components of the electric field within the metal are given by:

$$E_x^{metal} = E_0 \mathrm{e}^{i(k_x x - k_{z1}|z| - \omega t)} \tag{1.6a}$$

$$E_y^{metal} = 0 \tag{1.6b}$$

$$E_z^{metal} = E_0 \left(\frac{-k_x}{k_{z1}}\right) \mathrm{e}^{i(k_x x - k_{z1}|z| - \omega t)} \tag{1.6c}$$

and the components of the electric field within the dielectric are given by:

$$E_x^{dielectric} = E_0 \mathrm{e}^{i(k_x x - k_{z2}|z| - \omega t)} \tag{1.7a}$$

$$E_y^{dielectric} = 0 \tag{1.7b}$$

$$E_z^{dielectric} = E_0 \left(\frac{-\epsilon_1 k_x}{\epsilon_2 k_{z1}}\right) \mathrm{e}^{i(k_x x - k_{z2}|z| - \omega t)} \tag{1.7c}$$

where k_{z1} and ϵ_1 represent the wave vector and dielectric constant within the metal layer and k_{z2}

and ϵ_2 represent the wavevector and dielectric constant within the dielectric layer. For both sets of equations, k_x represents the component of the wave vector in the direction of propagation along the metal-dielectric interface. Similarly, k_z represents the component of the wave vector perpendicular to the metal-dielectric interface and from this, we obtain the decay length of the electro-magnetic field into the layers:

$$\hat{z} = \frac{1}{|k_z|} \tag{1.8}$$

By requiring continuity of the $\vec{E}$ and $\vec{B}$ fields at the interface between the two layers, we obtain the dispersion relation for a single metal-dielectric interface [71, 108]:

$$k_x = \frac{\omega}{c} n_{spp} \tag{1.9a}$$

$$k_{z1,2}^2 = \epsilon_{1,2} \left(\frac{\omega}{c}\right)^2 - k_x^2 \tag{1.9b}$$

where the effective surface plasmon index is given by:

$$n_{spp} = \sqrt{\frac{\epsilon_1 \epsilon_2}{\epsilon_1 + \epsilon_2}} \tag{1.10}$$

1.4.2 Metal Insulator Metal Waveguides

One of the benefits of coupling light from free space into surface plasmons, is that you can significantly reduce the wavelength of the light. Taking this design one step further, by placing a second metal layer above the dielectric layer as well as below, one can fabricate a metal-insulator-metal (MIM) waveguide. These structures allow extremely high modal confinement of light.

Dispersion calculations for the MIM geometry are reported in Appendix A and the results are reported here. For transverse-magnetic polarized light, the dispersion relations for MIM waveguides are given by:

$$\epsilon_2 k_{z1} + \epsilon_1 k_{z2} \begin{Bmatrix} \coth(k_{z1} d/2) \\ \tanh(k_{z1} d/2) \end{Bmatrix} = 0 \tag{1.11}$$

where d represents the thickness of the dielectric layer. A schematic of such a structure and a representative plot of the dispersion relation is shown in Figure 1.3. Seen in the dispersion diagram are the different plasmonic and photonic modes that would be supported within this structure over the visible spectrum as a function of the real part of k_x. As a reference, the light line for this structure is plotted as the dotted line, and the surface plasmon and bulk plasma frequencies are

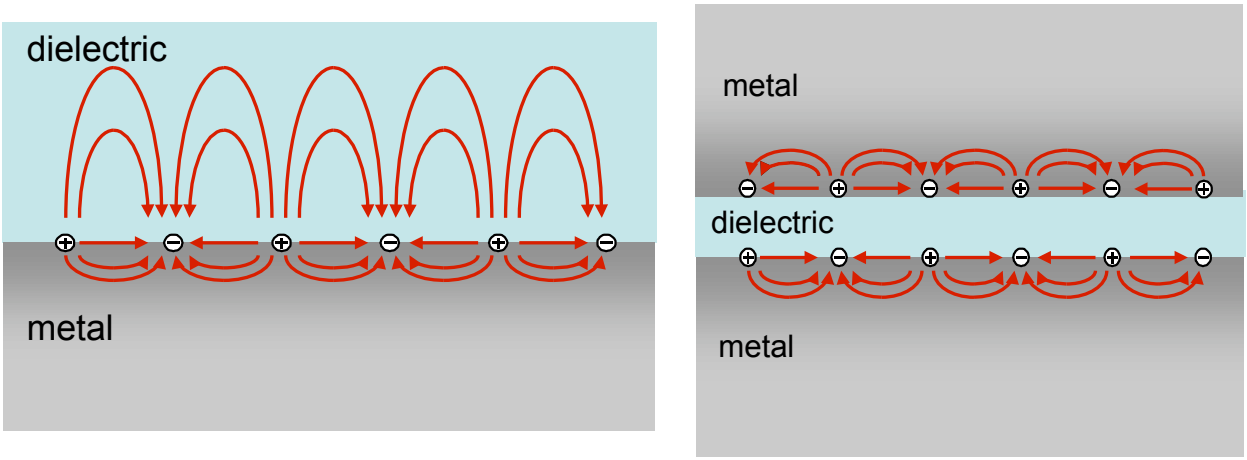

Figure 1.2. The figure on the left shows the electric field lines of a surface plasmon at a metal-dielectric interface. The figure on the right shows the same schematic for a metal-insulator-metal waveguide.

also labeled. This plot shows the existence of the plasmonic mode as well as one photonic mode within the structure. Here the plasmonic mode lies to the right of the light line because of the fact that this mode has a higher momentum than a free-space wave that would couple into it. In contrast, the photonic mode, whose momentum is strictly less than a free-space wave to which it would couple, lies to the left of the light line.

The phase and group velocities for these optical modes are defined by:

$$v_p = \frac{\omega}{k} \tag{1.12a}$$

$$v_g = \frac{\partial \omega}{\partial k} \tag{1.12b}$$

We can see that near the plasmon resonance in Figure 1.3, $v_g \to 0$, and this "slow wave" is characteristic of surface plasmons.

1.5 Scope of this Thesis

As the title suggests, the scope of this thesis is the design and fabrication of active MIM waveguides that support plasmonic and photonic modes. The idea is that by replacing the insulator layer with an active material and applying an electric field across the device, the output of the devices can be

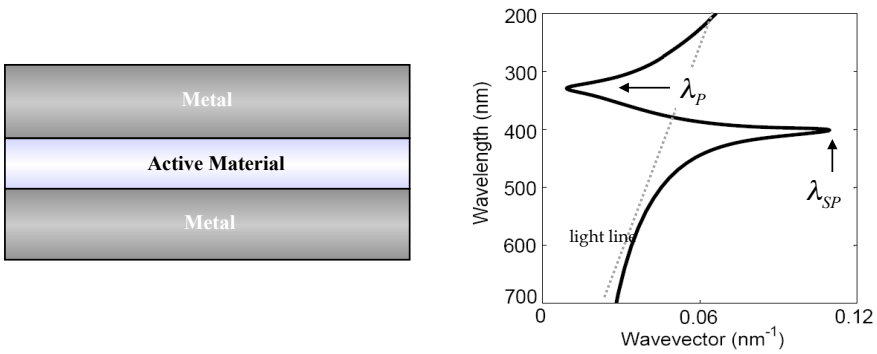

Figure 1.3. The figure on the left shows a generalized schematic of the semi-infinite metal-insulator-metal waveguide. The plot on the right shows a typical dispersion diagram for this type of structure. Both the plasma and surface plasmon resonances can be tuned over a wide range of the electromagnetic spectrum by changing the dimensions of and materials that make up the layers within the waveguide.

tuned across the visible and infrared portions of the electromagnetic spectrum.

By changing each of the materials in the three layer stack (Figure 1.4), as well as their relative thicknesses, the dispersion properties of the device as well as the resonance and filtering properties can be tuned over a wide range of the electromagnetic spectrum. In addition, by changing the dimensions of the in-coupling and out-coupling structures, as well as the distance between them, we can selectively access a large range of the different waveguide mode profiles that are present within the structure.

To this end, there are two main sections of the thesis. Each focuses on active MIM waveguides that utilize a different physical mechanism to induce a change in the region that supports the various optical modes. The first section looks at the utilizing electro-optic effect in lithium niobate to create tunable color filters, and the second section looks at modulating the carrier density distribution across the structure in n-type silicon and indium tin oxide to change the mode profiles within the waveguide.

1.5.1 Part I: Ferroelectric Slot Waveguides

Part I of this thesis deals with using ferroelectric materials as the active layer between the two metal cladding layers of the waveguide. The idea is to take advantage of the electro-optic effect in ferroelectric materials and change the index of refraction within the waveguide under an ap-

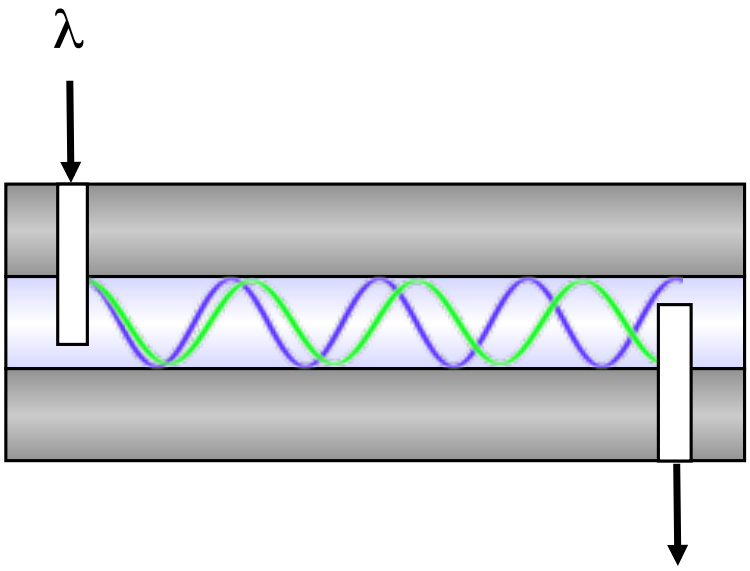

Figure 1.4. The schematic on the right shows a typical device that was fabricated using the basic metal-insulator-metal geometry.

plied electric field. In addition, all the ferroelectric layers used in this thesis were single crystal and obtained using ion-implantation induced layer transfer. This process has many benefits over conventional thin-film growth techniques and will be discussed in detail in Chapters 2, 3, and 4.

Chapter 2 is an overview of ferroelectric materials and the specific materials properties that enable them to perform the electro-optic switching discussed above. The chapter finishes with an overview of ion implantation induced layer transfer which is the method by which the thin film, single crystal ferroelectric layer are produced in this thesis. In Chapter 3, the ion-implantation induced layer transfer process is analyzed from a thermodynamic standpoint and the ion-implantation conditions required for layer transfer are determined. Assuming the sample has been properly ion-implanted, Chapter 4 analyzes the possible failure mechanisms that can occur in the layer transfered thin-film from the standpoint of thermal expansion-induced stress. The chapter then goes on to determine the necessary requirements for thin-film and substrate to ensure a coherent layer is transferred. This analysis is then done for the case of lithium niobate transferred onto a silicon substrate.

One of the largest difficulties in successful layer transfer is producing a strong, robust bond between the two materials in question. In Chapter 5, a new technique for metal bonding is introduced and analyzed. This process involves evaporating a layer of silver on both surfaces before

the layer transfer process, and during the course of the bonding/layer transfer step, Chapter 5 shows that diffusion bonding causes the two silver layers to become one, continuous layer. The last chapter in Part I, Chapter 6, looks at passive and active MIM waveguides with silicon nitride and lithium niobate in the optical channel. These devices are shown to naturally filter white light into individual colors based on the interference of the different optical modes within the dielectric layer. Full-field electromagnetic simulations show that these devices can preferentially couple to any of the primary colors and can tune the output color of the device with an applied field.

1.5.2 Part II: Semiconductor Slot Waveguides

Part II of this thesis deals with using two semiconductor materials (n-type silicon and indium tin oxide) as the active layer between the two metal cladding layers of the waveguide. Here the idea is to apply an electric field across the semiconductor layers and modulate the carrier distribution within the waveguide.

Chapter 7 examines a new type of plasmonic/photonic waveguide whose thickness is carefully chosen to support one plasmonic mode and exactly one photonic mode very close to cut-off. Through an extensive experimental analysis and full-field electromagnetic simulations, the device is show to behave like an MOS capacitor and with an applied field, push the photonic mode into cutoff.

Chapter 8 looks at changing the doping density within transparent conducting oxides (like indium tin oxide) to shift the plasma frequency into the near-infrared and visible wavelengths. The material is incorporated into an MOS structure similar to that in Chapter 7 and through extensive characterization using spectroscopic ellipsometry (Appendix C), the thin film stack is characterized with and without an applied electric field. The measurements show that when an accumulation layer is formed within the structure, the index of refraction within that layer is significantly changed and as a result, will change the optical modes supported in such a structure.